Leukemia & Lymphoma, September 2014; 55(9): 2151–2160

ISSN: 1042-8194 print / 1029-2403 online
DOI: 10.3109/10428194.2013.856008

informa
healthcare

ORIGINAL ARTICLE: RESEARCH

Enhanced anti-tumor activity of the glycoengineered type II CD20 antibody obinutuzumab (GA101) in combination with chemotherapy in xenograft models of human lymphoma

Frank Herting[1], Thomas Friess[1], Sabine Bader[1], Gunter Muth[1], Gabriele Hölzlwimmer[2], Natascha Rieder[2], Pablo Umana[3] & Christian Klein[3]

[1]*Discovery Oncology,* [2]*Pathology and Tissue Analytics, Pharma Research and Early Development (pRED), Roche Diagnostics GmbH, Penzberg, Germany and* [3]*Discovery Oncology, Pharma Research and Early Development (pRED), Discovery Oncology, Roche Glycart AG, Schlieren, Switzerland*

Abstract

Obinutuzumab (GA101) is a novel glycoengineered type II CD20 antibody in development for non-Hodgkin lymphoma. We compared the anti-tumor activity of obinutuzumab and rituximab in preclinical studies using subcutaneous Z138 and WSU-DLCL2 xenograft mouse models. Obinutuzumab and rituximab were assessed alone and in combination with bendamustine, fludarabine, chlorambucil, doxorubicin and cyclophosphamide/vincristine. Owing to strong single-agent efficacy in these models, suboptimal doses of obinutuzumab were applied to demonstrate a combination effect. Obinutuzumab plus bendamustine achieved superior tumor growth inhibition versus rituximab plus bendamustine and showed a statistically significant effect versus the respective single treatments. Combinations of obinutuzumab with fludarabine, chlorambucil or cyclophosphamide/vincristine demonstrated significantly superior activity to rituximab-based treatment. Obinutuzumab monotherapy was at least as effective as rituximab plus chemotherapy *in vivo*, and obinutuzumab plus chemotherapy was superior to the respective monotherapies. These data support further clinical investigation of obinutuzumab plus chemotherapy.

Keywords: GA101, obinutuzumab, rituximab, non-Hodgkin lymphom, glycoengineered, type II CD20 antibody

Introduction

The cell surface antigen CD20 is highly expressed on more than 90% of non-Hodgkin lymphoma (NHL) malignant B cells, and therefore represents an attractive target for the treatment of B-cell malignancies [1,2]. The type I anti-CD20 monoclonal antibody (mAb) rituximab (MabThera, Rituxan) was the first to be licensed for the treatment of cancer, and is now standard therapy for the initial treatment of diffuse large B-cell lymphoma (DLBCL), follicular lymphoma and chronic lymphocytic leukemia (CLL) [3,4]. In clinical practice, rituximab is administered in combination with various chemotherapy regimens, including CHOP (cyclophosphamide, doxorubicin, vincristine, prednisone), CVP (cyclophosphamide, vincristine, prednisone), bendamustine, chlorambucil, fludarabine, and FC (fludarabine, cyclophosphamide), resulting in enhanced activity and a substantial clinical benefit compared with chemotherapy alone [3,5]. Since its approval in 1997, rituximab has revolutionized the treatment of NHL, greatly improving 5-year and 10-year survival rates; however, despite this success, relapse remains a reality for many patients [6]. As a consequence, further research efforts have been directed at developing other monoclonal antibody-based therapies to prolong remission in patients with B-cell neoplasms.

Obinutuzumab (GA101) is a novel, glycoengineered, type II CD20 antibody in clinical development. Both obinutuzumab (GA101) and rituximab recognize overlapping CD20 epitopes, but in different ways; these differences in binding are thought to determine type I and II characteristics, such as more potent direct B-cell death induction by type II mAbs [7–9] and reduced CD20 internalization [10]. Another feature of obinutuzumab (GA101) is that the Fc region of the molecule has been glycoengineered to have an increased affinity for FcγRIII receptors expressed on natural killer (NK) cells, macrophages and monocytes, resulting in enhanced antibody-dependent cellular cytotoxicity (ADCC) [7]. Together, these structural modifications confer obinutuzumab (GA101) with enhanced immune effector functions and B-cell depleting activity compared with rituximab [7]. For example, in preclinical studies, obinutuzumab (GA101) demonstrated superior depletion of normal B cells (measured as CD19 + depletion)

Correspondence: Christian Klein, Discovery Oncology, Pharmaceutical Research and Early Development (pRED), Discovery Oncology, Roche Glycart AG, Wagistrasse 18, CH-8952 Schlieren, Switzerland. Tel: + 41-44-755-61-67. Fax: + 41-44-755-61-60. E-mail: christian.klein.ck1@roche.com

Received 5 July 2013; revised 8 October 2013; accepted 10 October 2013

from the blood of healthy volunteers [7], as well as of malignant B cells from the blood of patients with B-CLL [11], compared with rituximab. In addition, obinutuzumab (GA101) induced potent depletion of normal B cells from the peripheral blood and lymphoid organs of cynomolgus monkeys, as well as potent antitumoral efficacy in NHL xenograft models [7,12]. The promising *in vivo* anti-tumor activity of obinutuzumab (GA101) is supported by results from preclinical studies using subcutaneous (s.c.) xenograft models [7,12]. In the study by Mössner and colleagues, mice with established SU-DHL-4 DLBCL tumors were treated with obinutuzumab (GA101) 30 mg/kg every 7 days; complete tumor remission was achieved in 10 out of 10 mice and a survival rate of >90 days was reported in nine out of 10 mice. In contrast, none of the 10 mice treated with rituximab 30 mg/kg became tumor free [7]. Given its ability to induce significantly greater ADCC and direct cell death than rituximab, it has been suggested that obinutuzumab (GA101) may also have greater activity than rituximab in the clinical setting.

Here we describe the results of in vivo studies using Z138 mantle cell lymphoma (MCL) and WSU-DLCL2 DLBCL NHL xenograft models to evaluate the efficacy of obinutuzumab (GA101) alone and in combination with several chemotherapeutic agents. The experimental design of the studies took into account current clinical practice by evaluating (a) obinutuzumab (GA101) monotherapy in comparison with rituximab monotherapy and (b) the combination of either agent with the cytotoxic chemotherapies bendamustine, fludarabine, chlorambucil and cyclophosphamide/vincristine.

Materials and methods

Single-agent studies evaluated the single agent anti-tumor activity of obinutuzumab (GA101) and rituximab using the Z138 tumor xenograft. In three studies, the anti-tumor activity of obinutuzumab (GA101) or rituximab in combination with bendamustine, fludarabine or chlorambucil was compared with that of the respective single agents using the Z138 MCL tumor xenograft model in beige mice with severe combined immune deficiency (SCID). In the WSU-DLCL2 xenograft model, single-agent obinutuzumab (GA101) and rituximab were evaluated and compared with cyclophosphamide/vincristine/doxorubicin. Furthermore, the anti-tumor activity of obinutuzumab (GA101) and rituximab was evaluated alone and in combination with cyclophosphamide/vincristine in the WSU-DLCL2 lymphoma xenograft model.

Animals and xenograft tumor models

Four- to 8-week-old female SCID beige mice were obtained from Charles River (Sulzfeld, Germany). The animals were housed in the quarantine part of an animal facility and left to adapt to their new environment for 1 week before studies began. The mice were maintained under specific pathogen-free conditions in accordance with international guidelines (GV-Solas; Felasa; TierSchG), with daily cycles of 12 h of light/12 h of darkness; diet food (Altromin or Provimi Kliba) and water were provided *ad libitum*. The study protocols were reviewed and approved by the local government (Regierung von Oberbayern; registration number 211.2531.2-22/2003).

The Z138 human MCL cell lines were obtained from Roche Glycart AG (Schlieren, Switzerland) and were cultured under routine tissue culture conditions in Dulbecco's modified Eagle's medium (DMEM) supplemented with 10% fetal calf serum and L-glutamine (2 mM). WSU-DLCL2 lymphoma cells were sourced from Wayne State University School of Medicine (Detroit, MI) and were cultured in RPMI 1640 medium supplemented with 10% fetal bovine serum albumin and L-glutamine (2 mM). The cell cultures were maintained at 37°C in a water-saturated atmosphere at 5% CO_2. All cells were passaged maximally 25 times and between 88.6% and 98.0% viable at the point of transplant.

On the day of cell injection, the tumor cells were harvested from culture flasks (Greiner T 75), transferred into culture medium (50 mL), washed once and resuspended in phosphate buffered saline (PBS). After an additional washing with PBS, cell concentration was measured using a Vi-Cell™ (Cell Viability Analyzer; Beckman Coulter, Madison, WI). The tumor cell suspension was mixed carefully to reduce cell aggregation and kept on ice. Z138 lymphoma cells (5×10^6 cells per animal) and WSU-DLCL2 tumor cells (2×10^6 cells per animal) were injected s.c. in a volume of 50 µL PBS and 50 µL Matrigel™ into the right flank of SCID beige mice.

Dose selection

Doses of obinutuzumab (GA101) in the single-agent studies were selected based on similar doses of obinutuzumab (GA101) and rituximab used in previous preclinical experiments, where maximal efficacy was achieved with doses of 10–30 mg/kg (Mössner *et al.*, 2010; unpublished data). In the Z138 combination studies, suboptimal doses of obinutuzumab (GA101) and rituximab <10 mg/kg in terms of anti-tumor activity were applied to analyze potential additional or synergistic effects in combination with the various chemotherapeutic agents. The doses of the chemotherapeutic drugs bendamustine, fludarabine, chlorambucil and cyclophosphamide/vincristine/doxorubicin were selected based on published non-clinical data [13–17].

Study treatment and administration schedules

Animals in the control group in all experiments received vehicle alone, which was 0.9% sodium chloride solution (obtained from Fresenius Kabi). The administration volume was 10 mL/kg. Study drugs were obtained from commercial sources: obinutuzumab (GA101) and rituximab from Roche, bendamustine (Ribomustin) from Mundipharma, fludarabine and vincristine from Medac, cyclophosphamide (Endoxan) from Baxter Oncology and chlorambucil from Aspen Pharma. Nine to 27 days after tumor cell injection, animals were randomized into groups and treatment began in accordance with the study protocols for the individual experiments (Supplementary Table I to be found online at http://informahealthcare.com/doi/abs/10.3109/10428194.2013.856008).

Animal monitoring

Animals were assessed twice weekly for changes in health and body weight. Tumor dimensions were measured by

caliper on the staging day at the beginning of the treatment period and then twice weekly. Mice were sacrificed under general anesthesia by cervical dislocation on day 30 (single-agent_WSU-DLCL2_experiment 8), day 33 (combined bendamustine_Z138_experiment 5), day 41 (combined chlorambucil_Z138_experiment 7), day 43 (combined fludarabine_Z138_experiment 6), day 49 (single-agent_Z138_experiment 3) or at various time points from day 32 to day 66 (single-agent_Z138_experiments 1, 2 and 4 and single-agent/combination_WSU-DLCL2_experiment 9). Animals who met the following criteria before the relevant pre-specified time point were sacrificed prematurely: critical tumor mass of up to 4 g (or a diameter > 2 cm), body weight loss > 20% from baseline, tumor ulceration or poor general condition. Necropsy was performed, and the primary tumors were resected and weighed.

Determination of antibody serum levels

Serum samples were taken 1, 6, 24 and 72 h after first antibody injection from all treatment groups and from three animals at each time point. After collection, the samples were stirred gently and maintained on ice. Samples were centrifuged at 1000 × *g* for 10 min at 4°C and stored at − 20°C until analysis. A generic human immunoglobulin G (huIgG) assay was used for antibody determination.

The concentrations of antibodies in mouse sera were determined via enzyme linked immunosorbent assay (ELISA). A biotinylated monoclonal antibody against human Fcγ (mAb< hFcγ>-Bi) was bound to a streptavidin-coated microtiter plate in the first step. Serum samples and reference standards, respectively, were preincubated with digoxigenylated monoclonal antibody against human Fcγ (mAb< hFcγ>-Dig). The preincubated complexes were then bound to the immobilized mAb< hFcγ>-Bi and detected via anti-Dig-horseradish peroxidase antibody-conjugate. ABTS [2,2′-azino-bis(3-ethylbenzthiazoline-6-sulfonic acid)] solution was used as the substrate for horseradish peroxidase.

cell per FOV, + [slight] = 2–3, ++ [moderate] = 4–5, +++ [severe] = 6–9, ++++ [extreme] = ≥ 10), capsule formation, percentage necrosis and invasive growth.

For immunohistological staining, mouse monoclonal anti-human CD20 antibody (Dako; Clone L26) and mouse monoclonal antibody MCA2454 (Serotec; Clone LE-CD19), which recognizes human CD19 (single-agent/combination_WSU-DLCL2_experiment only), were used. The following immunohistological parameters were investigated: total CD20/CD19 expression (as staining intensity: [+] = very weak, + = weak, ++ = moderate, +++ = strong), estimation of the percentage of CD20/CD19-positive tumor cells compared with the total number of tumor cells, and the intracellular and intratumoral localization of CD20/CD19 expression.

Determination of response

Criteria used to determine anti-tumor activity differed somewhat between experiments. For all experiments, tumor volume (TV) and tumor control ratio (TCR) were calculated. For part of the experiments tumor growth inhibition (TGI) was reported. In addition, time-to-event or tumor growth delay (from day 35 to day 64) was assessed where required.

Estimation of TV

TV was calculated in accordance with the National Cancer Institute protocol [TV = (length × width^2)/2], where length and width are the long and short diameters, respectively, of tumor mass (mm) [18]. The calculation was performed from the staging day until study termination, and values were presented as mean (± SEM, standard error of mean).

Estimation of TGI

TV was used to calculate TGI during the treatment period using the following formula:

$$\text{TGI}\,(\%) = 100 - \frac{\text{median}\,[TV(treated)_{day\,z} - TV(treated)_{day\,x}]}{\text{median}\,[TV(respective\,control)_{day\,z} - TV(respective\,control)_{day\,x}]} \times 100$$

Histology and immunohistology

Changes in general histological parameters were studied on hematoxylin and eosin (H&E)-stained slides. CD20/CD19 immunohistochemistry analysis was performed on five of 10 animals per group in Z138 NHL xenografts (bendamustine combination in Z138) and on four of 10 animals per group in WSU-DLCL2 tumor xenografts (single-agent/combination study in WSU-DLCL2). At necropsy, primary tumors were excised and fixed in buffered formaldehyde solution (3.8%) and then embedded in Paraplast® (Thermo Scientific). For histopathological evaluation, sections were evaluated using H&E staining; various parameters were assessed, including rate of proliferation and apoptosis (by counting the number of mitotic figures or apoptotic cells at × 200 magnification in five fields of view [FOV] and subsequent semiquantitative scoring: [+] [minimal] = 1 average mitotic figure or apoptotic

Mean TV was used in place of median TV in this formula.

Each treatment group was compared with its respective vehicle control. $TV_{day\ z}$ represented TV for an individual animal at a defined study day (day *z*), and $TV_{day\,x}$ represented TV of an individual animal at the staging day (day *x*).

Correlation between tumor weight and TV

Tumors were weighed at necropsy, and the correlation coefficient *R* was calculated for TV and tumor weight.

Statistical analysis

Statistical analysis was conducted using either SAS-JMP version 7 or version 8.2, or TUMGRO (version 1.3) with SAS version 8.1 software (SAS Inc., Cary, NC). Data on primary tumor growth were analyzed statistically using non-parametric methods if the data showed asymmetrical behavior, or

parametric methods if normality of TV values was observed. Prior to this, data were baseline-corrected using TV at the start of treatment, based on differences, or if regression was observed for at least one animal, based on ratios. In a randomized two-sample design, the TCR and its two-sided parametric or non-parametric confidence interval (CI; 1–α) were estimated. For the parametric estimator, the following formula was used, along with Fieller's CI for ratios [19]:

$$\mathrm{TCR} = \frac{\bar{V}_{treated}}{\bar{V}_{control}}$$

where $\bar{V}$ is mean tumor volume.

For the non-parametric analysis, the TCR and its confidence limits were calculated as the median and quartiles of all pairwise ratios between animals of the analyzed treatment and control groups. Area under the curve (AUC) was estimated by the trapezoidal rule based on TV data starting from the day of treatment start. AUC was then converted to the standardized AUC (sAUC) to allow comparisons between animals that dropped out of the studies at different time points by the following formula:

$$\mathrm{sAUC} = \mathrm{AUC}/(\text{day of drop-out} - \text{day of treatment start})$$

For all experiments except the bendamustine combination in Z138, TV at last study day was considered as the analysis endpoint. Exceptions were studies with similar TV across treatment groups at the end of treatment when a considerable difference of growth curves was observed over the course of the study. In these cases, the sAUC was considered for analysis to reflect the different growth behavior.

For animals treated with the fludarabine combination in Z138, a time-to-event analysis was performed until day 43 after tumor cell inoculation to further compare the antitumor efficacy of obinutuzumab (GA101)/fludarabine combination therapy with rituximab plus fludarabine combination therapy. The critical tumor burden was set as baseline TV plus an offset of 500 mm^3. Treatment groups were compared using a pairwise version of the log-rank test. Animals that had not reached the critical tumor burden by day 43 were censored. In the single-agent/combination study in WSU-DLCL2, an equivalent analysis was performed using a critical tumor burden of 1000 mm^3.

Role of the funding source

F. Hoffmann-La Roche provided financial support for third-party writing assistance for this manuscript.

Results

Effect of single-agent obinutuzumab (GA101) or rituximab on growth of Z138 MCL xenografts

The dose-dependent efficacy of obinutuzumab (GA101) and its superiority over rituximab was demonstrated in the s.c. Z138 MCL xenograft model. In the first study, weekly dosing of obinutuzumab (GA101) at 10 mg/kg (every 7 days [q7d] ×4, intravenous [i.v.]) induced complete tumor remission and long-term survival (cures) in all treated animals, whereas rituximab administration was only able to induce complete tumor remissions in four of 10 animals. All animals treated with obinutuzumab (GA101) remained tumor free and survived until study termination (Figure 1).

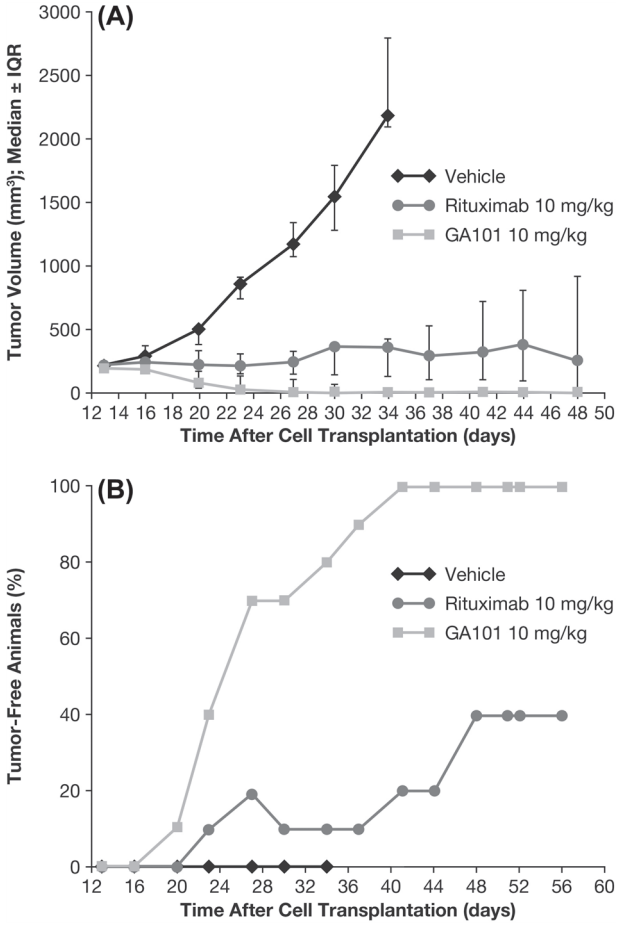

Figure 1. Tumor growth inhibition (TGI) and tumor-free animals in s.c. Z138 MCL model following 10 mg/kg obinutuzumab (GA101) or rituximab. IQR, interquartile range. Treatment of the s.c. Z138 MCL model with 10 mg/kg obinutuzumab or rituximab (q7d ×4, i.v.) was initiated when tumor reached an average size of 214 mm^3. (A) TGI until day 48, (B) number of tumor-free animals until day 56.

When obinutuzumab (GA101) and rituximab were compared at the higher dose of 30 mg/kg (q7d ×3, intraperitoneal [i.p.]), both antibodies induced complete tumor remission, but obinutuzumab (GA101) showed an earlier onset of tumor regression (Supplementary Figure 1 to be found online at http://informahealthcare.com/doi/abs/10.3109/10428194.2013.856008). While at study day 35, 100% of obinutuzumab-treated animals were tumor free, no tumor-free animals were observed in the rituximab group. Rituximab-treated mice showed tumor regression only on day 42, and no re-growth was observed after a 4-week observation period for both groups. Subsequently, in this model, four doses of 1, 10, 30 and 100 mg/kg (q7d ×4, i.v.) of obinutuzumab (GA101) and rituximab were evaluated. The aims of measuring trough levels in this experiment were to detect the drug serum levels achieved with the various dosages immediately prior to next drug administration and to examine these lowest values in the context of anti-tumor activity (and compare them with the efficacious concentrations determined *in vitro*). Such preclinical drug monitoring could also further support the pharmacokinetic/pharmacodynamic

models used to guide clinical study design. The efficacious dose of obinutuzumab (GA101) was reached, with 10 mg/kg corresponding to trough serum levels of approximately 100 µg/mL; however, with doses of obinutuzumab (GA101) 100 mg/kg corresponding to trough serum levels of 500–700 µg/mL, the efficacy in terms of kinetics of tumor regression could still be slightly enhanced (Supplementary Figures 2 and 3 to be found online at http://informahealthcare.com/doi/abs/10.3109/10428194.2013.856008).

In order to investigate whether the enhanced efficacy of obinutuzumab (GA101) is due to glycoengineering, an experiment using a non-glycoengineered, wild-type version of obinutuzumab (GA101) in the s.c. Z138 model was performed. Notably, the non-glycoengineered, wild-type version of obinutuzumab (GA101) at a dose of 10 mg/kg (q7d × 4, i.v.) was able to induce complete tumor remission with kinetics and number of tumor-free animals comparable to obinutuzumab (GA101) at the same dose. This indicates that in the s.c. Z138 model glycoengineering is not responsible for the superior efficacy of obinutuzumab (GA101) (Figure 2).

When obinutuzumab (GA101) was administered second line at a dose of 10 mg/kg (q7d × 4, i.p.) in animals bearing s.c. Z138 tumors previously treated with bendamustine, obinutuzumab (GA101) induced complete tumor remission in five of nine animals pretreated with vehicle control or with 2 mg/kg bendamustine (q1d × 4, i.p.) and was able to induce complete tumor remission in all animals pretreated with 6 or 12 mg/kg bendamustine (q1d × 4, i.p.) (nine of nine animals).

Effect of obinutuzumab (GA101) and rituximab in combination with chemotherapy on growth of Z138 MCL xenografts

One of the problems faced when testing obinutuzumab (GA101) in combination with chemotherapy in these models is the strong single-agent activity of obinutuzumab (GA101) resulting in complete tumor remission. Therefore, the effect of obinutuzumab (GA101) and rituximab in combination with the respective chemotherapy was evaluated in the Z138 model using a suboptimal dose of 1 mg/kg, which is below the dose with optimal efficacy of ≥ 10 mg/kg. Compared with control animals (vehicle group), TV at the end of study was decreased in mice treated with obinutuzumab (GA101) or rituximab monotherapy, obinutuzumab (GA101) in combination with bendamustine, fludarabine or chlorambucil, or rituximab in

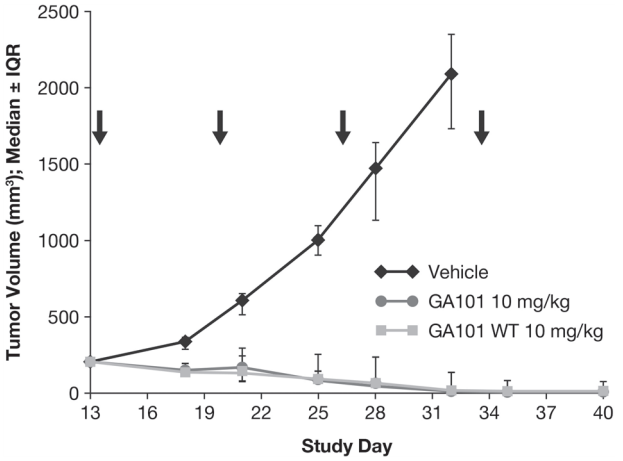

Figure 2. Effect of CD20 antibody treatment with 10 mg/kg glycoengineered and wild-type (WT) obinutuzumab (GA101) (q7d × 4) on tumor growth (day 40). IQR, interquartile range.

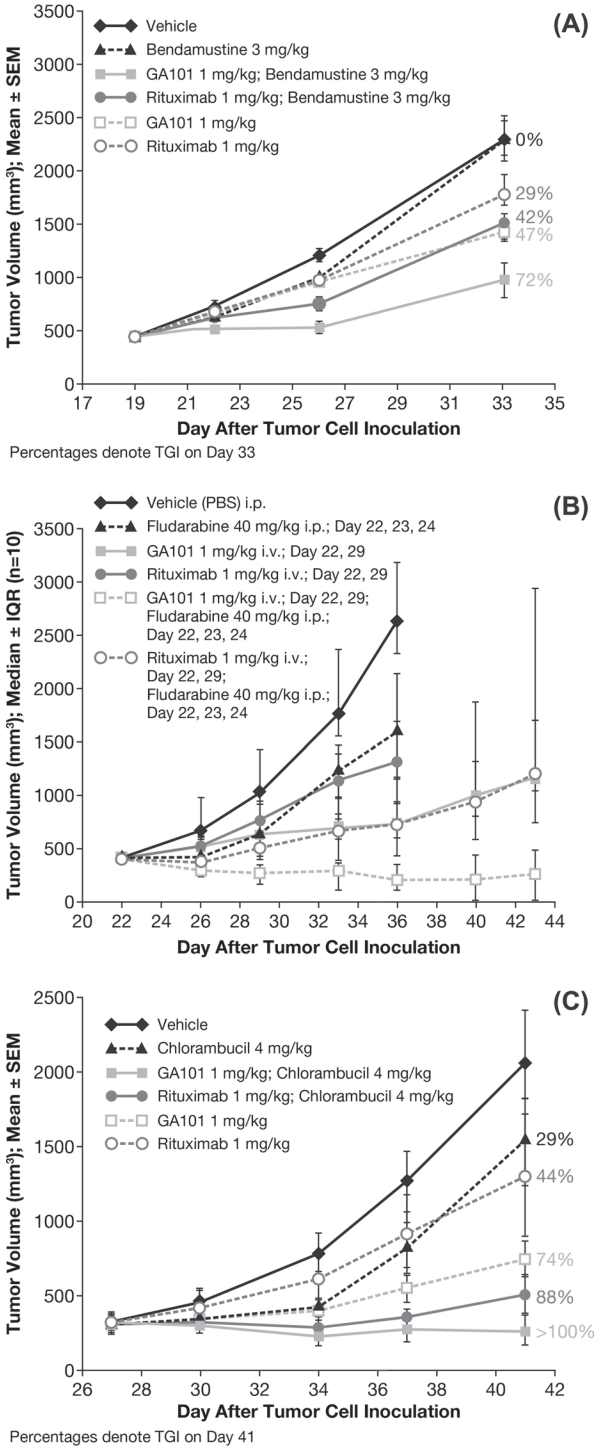

Figure 3. Effect of treatment on tumor cell growth in subcutaneously implanted Z138 MCL xenografts treated with: (A) obinutuzumab (GA101) (1 mg/kg days 19, 26, i.p.) or rituximab (1 mg/kg days 19, 26, i.p.) in combination with bendamustine (3 mg/kg days 19, 20, 21, 22, i.p.) or each agent as monotherapy; (B) obinutuzumab (GA101) (1 mg/kg days 22, 29, i.p.) or rituximab (1 mg/kg days 22, 29, i.v.) in combination with fludarabine (40 mg/kg days 22, 23, 24, i.p.) or each agent as monotherapy; (C) obinutuzumab (GA101) (1 mg/kg days 27, 34, i.v.) or rituximab (1 mg/kg days 27, 34, i.v.) in combination with chlorambucil (4 mg/kg days 27, 28, 29, i.p.) or each agent as monotherapy. IQR, interquartile range; PBS, phosphate buffered saline; SEM, standard error of mean; TGI, tumor growth inhibition.

combination with bendamustine, fludarabine, or chlorambucil [Figures 3(A)–3(C)]. Treatment with obinutuzumab (GA101) alone, or in combination with any of the three chemotherapeutic agents, inhibited tumor growth in a superior manner compared with the equivalent treatment with rituximab (Table I). Moreover, combinations of obinutuzumab (GA101) with fludarabine and with chlorambucil showed tumor regression, as indicated by a TGI value $>100\%$.

For the bendamustine combination in the Z138 model, calculation of TCR revealed statistically significant tumor inhibition for all treatment groups, except bendamustine monotherapy (3 mg/kg days 19, 20, 21, 22, i.p.; Table I and Figure 3). Furthermore, obinutuzumab (GA101) (1 mg/kg days 19, 20, i.p.) plus bendamustine (1 mg/kg days 19, 26, i.p.) demonstrated an enhanced and statistically significant TGI effect compared with single-agent treatment with obinutuzumab (GA101), rituximab (1 mg/kg days 19, 26, i.p.) or bendamustine ($p<0.001$, Tukey–Kramer test). By contrast, the TGI effect of rituximab plus bendamustine was not statistically significant compared with that of the three monotherapies.

For the fludarabine combination in the Z138 model, combination therapy comprising obinutuzumab (GA101)

Table I. Tumor control ratio (TCR, 95% confidence interval [CI]) and percentage tumor growth inhibition (TGI).

	TCR*	95% CI (vs. controls)	TGI (%)
Single-agent studies in Z138 xenograft			
Single-agent obinutuzumab (GA101) or rituximab			
Rituximab 10 mg/kg	0.15	0.00–0.36	92
Obinutuzumab (GA101) 10 mg/kg	0.00	0.00–0.21	>100
Single-agent obinutuxumab (GA101) or rituximab			
Rituximab 1 mg/kg	0.65	0.48–0.86	54
Rituximab 10 mg/kg	0.37	0.31–0.48	77
Rituximab 30 mg/kg	0.32	0.19–0.45	79
Rituximab 100 mg/kg	0.31	0.22–0.41	89
Obinutuzumab (GA101) 1 mg/kg	0.55	0.43–0.81	53
Obinutuzumab (GA101) 10 mg/kg	0.24	0.11–0.37	88
Obinutuzumab (GA101) 30 mg/kg	0.25	0.18–0.34	95
Obinutuzumab (GA101) 100 mg/kg	0.17	0.12–0.23	104
Single-agent obinutuzumab (GA101)			
Obinutuzumab (GA101) 10 mg/kg	0.00	0.00–0.03	>100
Obinutuzumab (GA101) WT 10 mg/kg	0.01	0.00–0.11	>100
Combination studies in Z138 xenograft			
Bendamustine combination			
Obinutuzumab (GA101) 1 mg/kg	0.72	0.59–0.86	47
Rituximab 1 mg/kg	0.78	0.65–0.93	29
Bendamustine 3 mg/kg	0.90	0.76–1.06	0
Obinutuzumab (GA101) 1 mg/kg + bendamustine 3 mg/kg	0.46	0.34–0.59	72
Rituximab 1 mg/kg + bendamustine 3 mg/kg	0.67	0.54–0.81	42
Fludarabine combination			
Obinutuzumab (GA101) 1 mg/kg	0.25	0.12–0.42	86
Rituximab 1 mg/kg	0.45	0.24–0.72	60
Fludarabine 40 mg/kg	0.59	0.36–0.98	50
Obinutuzumab (GA101) 1 mg/kg + fludarabine 40 mg/kg	0.07	0.00–0.16	>100
Rituximab 1 mg/kg + fludarabine 40 mg/kg	0.28	0.12–0.57	85
Chlorambucil combination			
Obinutuzumab (GA101) 1 mg/kg	0.39	0.20–0.60	74
Rituximab 1 mg/kg	0.53	0.34–0.76	44
Chlorambucil 4 mg/kg	0.77	0.56–1.03	29
Obinutuzumab (GA101) 1 mg/kg + chlorambucil 4 mg/kg	0.10	−0.08–0.30	>100
Rituximab 1 mg/kg + chlorambucil 4 mg/kg	0.23	0.05–0.43	88
Single-agent studies in WSU-DLCL2 xenograft			
Single-agent obinutuzumab (GA101) or cyclophosphamide/vincristine/doxorubicin			
Obinutuzumab (GA101) 30 mg/kg	0.20	0.07–0.50	81
Obinutuzumab (GA101) 100 mg/kg	0.24	0.11–0.47	75
Cyclophosphamide/vincristine 25/0.25 mg/kg	0.47	0.29–0.77	56
Doxorubicin	0.41	0.21–0.80	58
Cyclophosphamide/vincristine/doxorubicin	0.17	0.10–0.60	84
Combined studies in WSU-DLCL2 xenograft			
Cyclophosphamide/vincristine combination			
Obinutuzumab (GA101) 30 mg/kg	0.26	0.17–0.38	NC
Rituximab 30 mg/kg	0.41	0.31–0.59	NC
CYC/VINC 25/0.25 mg/kg	0.49	0.39–0.66	NC
Obinutuzumab (GA101) 30 mg/kg + CYC/VINC 25/0.25 mg/kg	0.22	0.17–0.31	NC
Rituximab 30 mg/kg + CYC/VINC 25/0.25 mg/kg	0.28	0.22–0.38	NC
CYC/VINC 25/0.25 mg/kg, then obinutuzumab (GA101) 30 mg/kg	0.61	0.42–0.85	NC
CYC/VINC 25/0.25 mg/kg, then rituximab 30 mg/kg	0.59	0.41–0.89	NC
CYC/VINC 25/0.25 mg/kg, then CYC/VINC 25/0.25 mg/kg + obinutuzumab (GA101) 30 mg/kg	0.49	0.40–0.67	NC
CYC/VINC 25/0.25 mg/kg, then CYC/VINC 25/0.25 mg/kg + rituximab 30 mg/kg	0.49	0.41–0.66	NC

WT, wild-type non-glycoengineered; CYC, cyclophosphamide; VINC, vincristine; NC, not calculated; sAUC, standardized AUC; TV, tumor volume.
*TCR values based on calculation of sAUC (single-agent obinutuzumab [GA101] or rituximab 10 mg/kg in Z138 xenograft) or endpoint analysis (day 36, 41, 35 or 38 for fludarabine combination in Z138 xenograft, chlorambucil combination in Z138 xenograft, single-agent/combination in WSU-DLCL2 and bendamustine combination in Z138 xenograft, respectively). Single-agent obinutuzumab (GA101) or rituximab 30 mg/kg i.p. is not included in this table as TV was calculated for that experiment, but not TCR or TGI.

(1 mg/kg days 22, 29, i.p.) plus fludarabine (40 mg/kg days 22, 23, 24, i.p.) was significantly superior to obinutuzumab (GA101) monotherapy and the rituximab (1 mg/kg days 22, 29, i.v.) plus fludarabine combination therapy in terms of TGI on day 36. TCR was 0.07 for obinutuzumab (GA101) plus fludarabine compared with 0.25 for obinutuzumab (GA101) alone. Median time-to-event was not reached in the obinutuzumab (GA101) plus fludarabine group and was 39.5 days in the rituximab plus fludarabine group (Figure 4).

For the fludarabine combination in Z138 and the single-agent/combination study in WSU-DLCL2, the vehicle group dropped out of the experiment at an early time point when the maximum benefit of treatment had only partially been achieved. For this reason, tumor growth data were converted into time-to-event data, where an event was defined as the time point when a critical tumor burden had been reached. A standard least-squares model was used to fit the individual tumor growth curves. Experiment-specific critical tumor burden values that most animals had reached were chosen to avoid too many censorings, while at the same time ensuring sufficient discrimination between groups. In terms of time-to-event, the superiority of the obinutuzumab (GA101) plus fludarabine combination compared with rituximab plus fludarabine was statistically significant ($p = 0.0023$). The superiority of obinutuzumab (GA101)–fludarabine combination therapy compared with obinutuzumab (GA101) monotherapy or rituximab–fludarabine combination therapy was further supported by the presence of three tumor-free animals on day 43 in the obinutuzumab (GA101) plus fludarabine group. In comparison, one animal was tumor free in the obinutuzumab (GA101) monotherapy group, and none of the animals treated with rituximab plus fludarabine were tumor free. In the fludarabine experiment, the vehicle, fludarabine and rituximab monotherapy treatment groups were terminated early (on day 36 after tumor cell inoculation) because individual tumors met the termination criteria.

For the chlorambucil combination in the Z138 model, combination treatment with obinutuzumab (GA101) (1 mg/kg days 27, 34, i.v.) and chlorambucil (4 mg/kg days 27, 28, 29, i.p.) resulted in tumor regression, whereas rituximab (1 mg/kg days 27, 34, i.v.) plus chlorambucil yielded a TGI of just 88%. Each of the treatments was statistically significant compared with the vehicle-treated group except for the monotherapy with chlorambucil group. Each of the combination treatments was statistically significant compared with rituximab monotherapy but was not significant when compared with obinutuzumab (GA101) monotherapy.

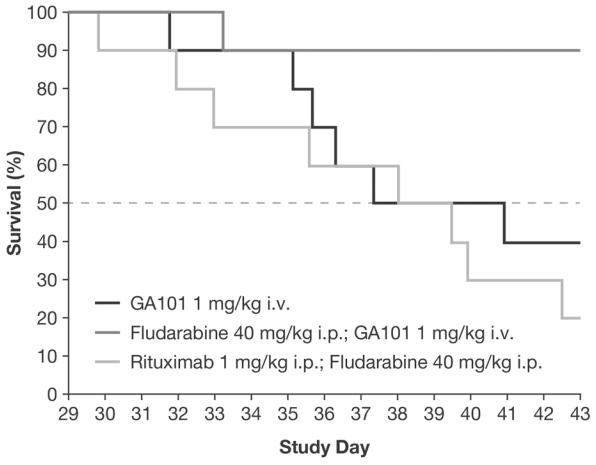

Figure 4. Kaplan–Meier curves for time-to-event until day 43 in s.c. implanted Z138 MCL xenografts treated with obinutuzumab (GA101) monotherapy, obinutuzumab (GA101)/fludarabine combination therapy, and rituximab plus fludarabine combination therapy.

Effect of single-agent obinutuzumab (GA101) on growth of WSU-DLCL2 xenografts

The WSU-DLCL2 model was found to be less responsive to anti-CD20 antibody therapy. In the SC WSU-DLCL2 model, obinutuzumab (GA101) demonstrated single-agent efficacy at doses of 30 and 100 mg/kg (q7d × 3, i.v.), resulting in TCR values of 0.2 (95% CI, 0.07–0.50) and 0.24 (0.11–0.47), corresponding to TGI of 81% or 75%, respectively. Therefore, 30 mg/kg obinutuzumab (GA101) corresponding to trough levels of 223 μg/mL appeared to mediate maximal effect in the WSU-DLCL2 model. Lower doses of obinutuzumab and rituximab resulted in inferior control of tumor growth (data not shown).

Effect of obinutuzumab (GA101) and rituximab in combination with cyclophosphamide/vincristine on growth of WSU-DLCL2 xenografts

During the 8-week treatment period for the single-agent/combination study in the WSU-DLCL2 model (treatment initiation to study termination), the greatest anti-tumor activity was observed with the combination of obinutuzumab (GA101) or rituximab plus cyclophosphamide/vincristine (Figure 5). Second-line treatment with cyclophosphamide/vincristine followed by obinutuzumab (GA101), or rituximab monotherapy, or their combination with cyclophosphamide/vincristine was not associated with an increase in anti-tumor activity compared with obinutuzumab (GA101) alone until day 50, or with rituximab until day 38 after tumor cell inoculation. Calculation of the TCR indicated that anti-tumor activity was maximal on day 35, with obinutuzumab (GA101) plus cyclophosphamide/vincristine (TCR = 0.22) followed by obinutuzumab (GA101) alone (TCR = 0.26) and rituximab plus cyclophosphamide/vincristine (TCR = 0.28) (Table I). Furthermore, at study termination (day 64), the combination of obinutuzumab (GA101) plus cyclophosphamide/vincristine was statistically superior to rituximab plus cyclophosphamide/vincristine in terms of anti-tumor activity (TCR 0.63; 95% CI, 0.47–0.85).

Kaplan–Meier estimates revealed superior tumor growth delay in terms of the survival endpoint (tumor burden volume of 1000 mm^3) for obinutuzumab (GA101) plus cyclophosphamide/vincristine versus rituximab plus cyclophosphamide/vincristine (Figure 5).

Histology

Tumors analyzed from Z138 xenografts showed evidence of cellular and nuclear polymorphism, an extreme rate of proliferation (mean of ≥ 10 mitotic figures per FOV) and a severe rate of apoptosis (mean of 6–9 apoptotic cells per FOV). A representative panel from human mantle cell Z138 tumor-bearing animals is shown in Figure 6. Compared with controls, tumors from mice treated with obinutuzumab (GA101) or rituximab alone showed improved tumor demarcation,

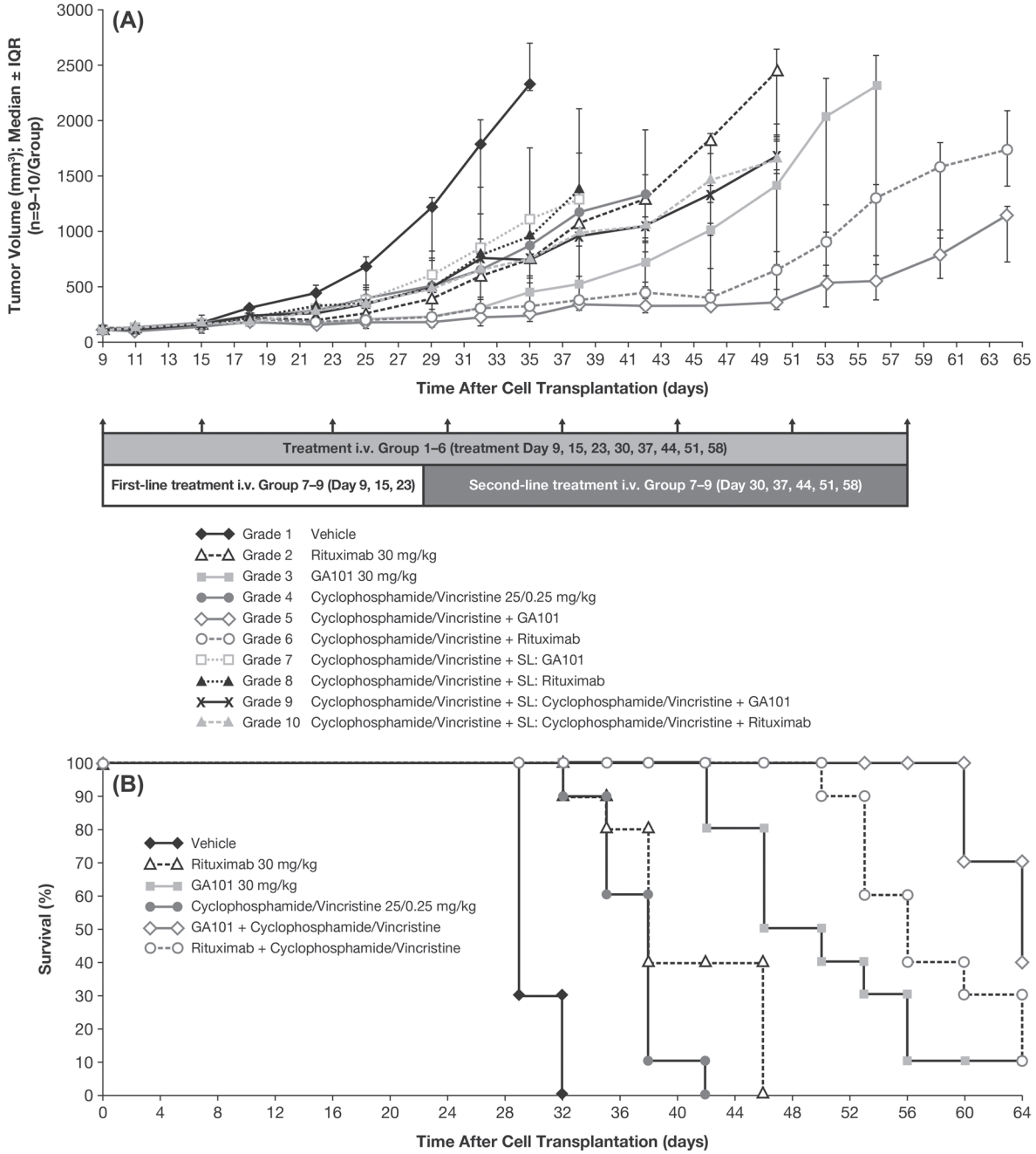

Figure 5. Effect of treatment on (A) tumor cell growth and (B) Kaplan–Meier estimate of survival in s.c. implanted WSU-DLCL2 lymphoma xenografts treated with obinutuzumab (GA101) or rituximab in combination with cyclophosphamide/vincristine or as monotherapy; survival endpoint was defined as tumor burden volume of 1000 mm^3. IQR, interquartile range.

with increased thickness of the surrounding fibrous capsule. Additionally, an increase in degenerative and apoptotic tumor cells in the tumor periphery was observed in H&E-stained sections. These morphological changes were enhanced after the addition of bendamustine to obinutuzumab (GA101) or rituximab (Figure 6). No differences in histopathological parameters were observed between the bendamustine monotherapy and vehicle treatment groups. CD20 immunohistochemical staining was strong and membrane-bound in almost all (>95%) tumor cells; there were no marked differences in CD20 expression between the different treatment groups or compared with vehicle-treated tumors.

Histological examination of excised WSU-DLCL2 tumors revealed diffuse NHL with a mixed population of large and intermediate cells with minimal capsule formation and an extreme/severe rate of proliferation and apoptosis (mean of 6–10 mitotic figures or apoptotic cells per FOV, respectively). Compared with vehicle-treated animals (strong membrane-bound expression of CD20 in >95% of tumor cells and moderate-to-strong membrane-associated expression of CD19 in >90% of tumor cells), tumors from mice treated with cyclophosphamide/vincristine in combination with obinutuzumab (GA101) had slightly reduced CD20 and CD19 expression (70–80% of tumor cells for CD20 and 50–70% for CD19) and a moderate decrease in the rate of proliferation. In contrast, tumors from animals treated with cyclophosphamide/vincristine alone or in combination with rituximab showed no change in histological parameters or

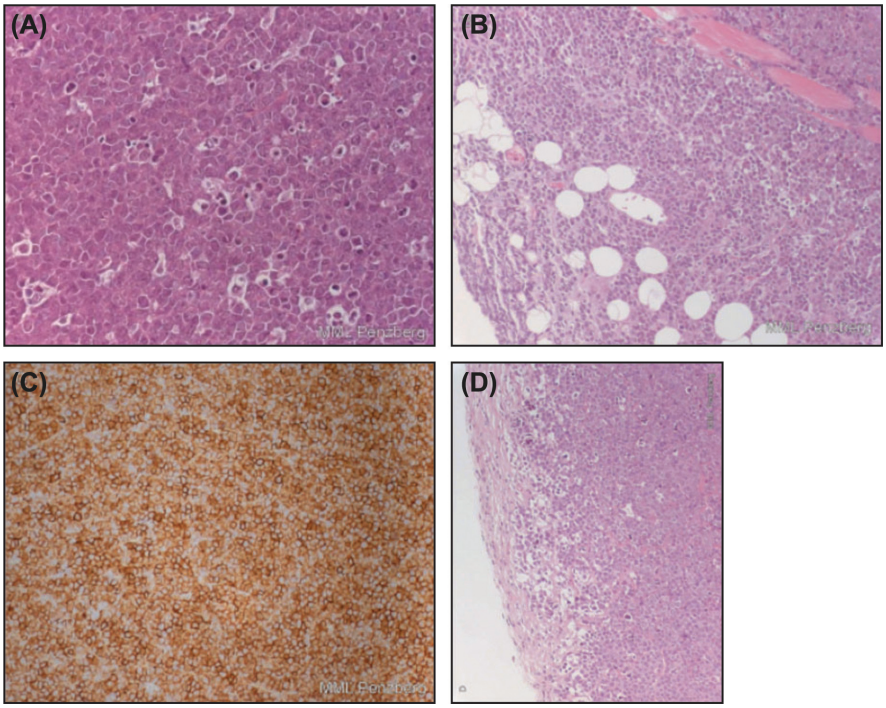

Figure 6. Tumor panels from Z138 tumor-bearing mice showing mantle cell NHL of Z138 human cell line: (A) (× 400 hematoxylin and eosin [H&E]) shows "starry sky" pattern as a result of apoptosis and phagocytosis; (B) (× 100 H&E) highlights infiltrative growth into surrounding subcutaneous tissue (muscle and fat), lacking distinct encapsulation (left; #101), respectively, with formation of a thin tumor-surrounding capsule of tumors of vehicle-treated mice (right, #102); (C) (× 200 CD20) shows strong membrane-bound CD20 expression in almost all MCL cells; (D) (× 100 H&E) demonstrates improved demarcation with increased capsule thickness after treatment with obinutuzumab (GA101) and bendamustine (left, #501) or after treatment with rituximab and bendamustine (right, #602). Note the small rim in the periphery of the tumor with increased vacuolated/degenerative and apoptotic tumor cells.

CD20 expression but a slight decrease in CD19 expression (70–80% of tumor cells stained moderate-to-strong) versus tumors from vehicle-treated mice. Compared with tumors from vehicle-treated animals, there was no distinct difference in the size of tumors from antibody-treated animals.

Discussion

These preclinical studies were designed to evaluate the anti-tumor activity of the type II glycoengineered anti-CD20 antibody obinutuzumab (GA101) versus that of rituximab when used alone or in combination with chemotherapeutic agents currently used in the treatment of hematologic malignancies. Our findings suggest that single-agent obinutuzumab (GA101) appears as effective as the combination of rituximab with chemotherapy in the preclinical setting. Furthermore, when combined with bendamustine, fludarabine, chlorambucil or cyclophosphamide/vincristine, obinutuzumab (GA101) has greater anti-tumor activity than rituximab plus chemotherapy. The clear superiority of the combination of obinutuzumab (GA101) plus fludarabine was further supported by evidence of complete tumor regression in three animals. In contrast, only one animal in the obinutuzumab (GA101) monotherapy group, and no animals in the rituximab plus fludarabine group were tumor free. The combination of obinutuzumab (GA101) plus bendamustine demonstrated an enhanced TGI effect compared with single-agent treatment with obinutuzumab (GA101), rituximab or bendamustine, while obinutuzumab (GA101) plus chlorambucil resulted in tumor regression, compared with a TGI of only 88% for rituximab plus chlorambucil. Together these findings provide strong evidence to suggest that the therapeutic response to chemotherapy may be enhanced by the addition of obinutuzumab (GA101).

Interestingly, second-line treatment schedules comprising three administrations of cyclophosphamide/vincristine followed by treatment with obinutuzumab (GA101) or rituximab alone or their combination each with cyclophosphamide/vincristine in the WSU-DLCL2 model did not demonstrate any improvement in anti-tumor activity compared with obinutuzumab (GA101) or rituximab alone until considerably late in the study (5–7 weeks after tumor cell inoculation). This underscores the importance of starting treatment with rituximab or obinutuzumab (GA101) in combination with chemotherapy to achieve optimal efficacy in this tumor model.

In the single-agent/combination study in the WSU-DLCL2 model, the doses of obinutuzumab (GA101), rituximab and cyclophosphamide/vincristine used were based on published data [13] and/or were selected based on previous experiments using mice bearing WSU-DLCL2 tumors. In the bendamustine and chlorambucil combination studies, we selected suboptimal doses of 1 mg/kg for obinutuzumab (GA101) and rituximab, and 3 mg/kg and 4 mg/kg for bendamustine and chlorambucil, respectively, to induce a moderate antitumor effect against NHL xenografts and thus allow evaluation of any enhanced effects with the combination of treatments. These effects were observed in both studies, where the combination of obinutuzumab (GA101) with chemotherapy achieved statistically significantly greater inhibition of tumor growth (as measured by percent TGI) compared with the combination

of rituximab and chemotherapy or obinutuzumab (GA101) monotherapy. The same suboptimal doses of obinutuzumab (GA101) and rituximab were used in combination with fludarabine in the Z138 model; however, fludarabine was administered at a maximum effective dose of 40 mg/kg, as this dose had yielded moderate anti-tumor activity in a previous preclinical study evaluating its anti-tumor activity against a human multiple myeloma xenograft [14].

The independent nature of the studies and their somewhat differing methodologies precludes direct comparison of the anti-tumor activity of the different obinutuzumab (GA101) combination chemotherapy regimens. However, TGI values for the different obinutuzumab (GA101) combination regimens suggest that TGI was greatest with obinutuzumab (GA101) plus fludarabine and obinutuzumab (GA101) plus chlorambucil (i.e. TGI was $>100\%$ with these combinations). In addition, although not designed to assess safety owing to lack of cross-reactivity with murine CD20, it is worth noting that there were no safety alerts in any of the studies.

Histological analysis of tumors treated with obinutuzumab (GA101) and rituximab provided some evidence of enhanced numbers of dying/apoptotic cells, as well as a moderate decrease in the rate of proliferation; however, based on these data, no clear conclusions about the mechanism of action responsible for the superior antitumor activity of obinutuzumab can be drawn. Experiments using a non-glycoengineered, wild-type version of obinutuzumab (GA101) indicate, however, that the superior efficacy in these xenograft models in SCID beige mice is not related to enhanced ADCC induction, but rather to type II-mediated mechanisms such as cell death induction and/or reduced CD20 internalization in combination with the effector function of a non-glycoengineered wild-type IgG1 antibody [10].

Notably, drug administration was initiated at a late stage of tumor development when established tumors had been formed. The consequent high level of tumor aggressiveness potentially minimized the likelihood of therapeutic anti-tumor activity; however, obinutuzumab (GA101) demonstrated highly promising *in vivo* anti-tumor activity when administered as monotherapy or when used in combination with chemotherapy.

In conclusion, the results of the present experiments using NHL xenograft models show that obinutuzumab (GA101) works in concert with classical chemotherapeutic agents and that these combinations are superior to respective combinations with rituximab. Although preclinical studies provide only a limited indication of the potential clinical efficacy of obinutuzumab (GA101), the results of these studies have potentially important implications for the design of future clinical trials evaluating obinutuzumab (GA101) in the treatment of hematologic malignancies. In addition, they lend further support to the ongoing clinical investigation of this anti-CD20 antibody in combination with chemotherapy for the treatment of NHL.

Supplementary material available online

Supplementary figures showing further results and tables showing treatment schedules.

Potential conflict of interest: Disclosure forms provided by the authors are available with the full text of this article at www.informahealthcare.com/lal.

References

[1] Nadler LM, Ritz J, Hardy R, et al. A unique cell surface antigen identifying lymphoid malignancies of B cell origin. J Clin Invest 1981;67:134–140.
[2] Anderson KC, Bates MP, Slaughenhoupt BL, et al. Expression of human B cell-associated antigens on leukemias and lymphomas:a model of human B cell differentiation. Blood 1984;63:1424–1433.
[3] Hagemeister F. Rituximab for the treatment of non-Hodgkin's lymphoma and chronic lymphocytic leukaemia. Drugs 2010;70: 261–272.
[4] Maloney D. Anti-CD20 antibody therapy for B-cell lymphomas. N Engl J Med 2012;366:2008–2016.
[5] National Comprehensive Cancer Network. NCCN Clinical Practice Guidelines in oncology. Non-Hodgkin's lymphomas V1.2013. Available from: http://www.nccn.org/
[6] Tilly H, Zelenetz A. Treatment of follicular lymphoma: current status. Leuk Lymphoma 2008;49(Suppl. 1):7–17.
[7] Mössner E, Brünker P, Moser S, et al. Increasing the efficacy of CD20 antibody therapy through the engineering of a new type II anti-CD20 antibody with enhanced direct and immune effector cell-mediated B-cell cytotoxicity. Blood 2010;115:4393–4402.
[8] Honeychurch J, Alduajj W, Azizyan M, et al. Antibody-induced nonapoptotic cell death in human lymphoma and leukemia cells is mediated through a novel reactive oxygen species-dependent pathway. Blood 2012;119:3523–3533.
[9] Niederfellner G, Lammens A, Mundigl O, et al. Epitope characterization and crystal structure of GA101 provide insight into the molecular basis for type I/II distinction of CD20 antibodies. Blood 2011;118:358–367.
[10] Lim SH, Vaughan AT, Ashton-Key M, et al. Fc gamma receptor IIb on target B cells promotes rituximab internalization and reduces clinical efficacy. Blood 2011;118:2530–2540.
[11] Patz M, Isaeva P, Forcob N, et al. Comparison of the in vitro effects of the anti-CD20 antibodies rituximab and GA101 on chronic lymphocytic leukaemia cells. Br J Haematol 2011;152:295–306.
[12] Dalle S, Reslan L, Besseyre de Horts T, et al. Preclinical studies on the mechanism of action and the anti-lymphoma activity of the novel anti-CD20 antibody GA101. Mol Cancer Ther 2011;10: 178–185.
[13] Mohammad RM, Wall NR, Dutcher JA, et al. The addition of bryostatin 1 to cyclophosphamide, doxorubicin, vincristine, and prednisone (CHOP) chemotherapy improves response in a CHOP-resistant human diffuse large cell lymphoma xenograft model. Clin Cancer Res 2000;6:4950–4956.
[14] Meng H, Yang C, Ni W, et al. Antitumor activity of fludarabine against human multiple myeloma in vitro and in vivo. Eur J Haematol 2007;79:486–493.
[15] Wiedmann M, Zeh J, Schoppmeyer K, et al. A new approach to the treatment of advanced hepatocellular carcinoma? J Chemother 2008;20:112–118.
[16] Kratz F, Beyer U, Roth T, et al. Albumin conjugates of the anticancer drug chlorambucil:synthesis, characterization, and in vitro efficacy. Arch Pharm Pharm Med Chem 1998;331:47–53.
[17] Tanaka O, Yoshioka N, Yoshioka T, et al. Effects of chlorambucil on the brain development in mice during post-neurulation period. Congenit Anom (Kyoto) 1991;31:141–152.
[18] Corbett TH, Valeriote F, LoRusso P, et al. In vivo methods for screening and preclinical testing:use of rodent solid tumors for drug discovery. In: Teicher BA, editor. Anticancer drug development guide. Preclinical screening, clinical trials and approval. Totowa, NJ: Humana Press; 1997. pp. 75–99.
[19] Fieller E. Some problems in interval estimation. J R Stat Soc 1954;B16:175–185.